The Syntheses and Luminescent Properties of Eu^{III} and Tb^{III} Cryptates in Solution

Qiu-Yun Chen,[a] Chang-Jian Feng,[a] Qin-Hui Luo,*[a] Chun-Ying Duan,[a] Xin-Sheng Yu,[a] and De-Jun Liu[a]

Keywords: Europium / Lanthanides / Cryptands / Luminescence / Mass spectrometry

The syntheses, characterization and luminescent properties of europium(III) and terbium(III) cryptates synthesized by [2+3] condensation of tris(2-aminoethyl)amine with 2,6-diformyl-4-R-phenol (R = Cl, F, *t*Bu) in the presence of Eu^{3+} or Tb^{3+} have been reported. The crystal structure of the europium cryptate (R = Cl) shows that the coordination number of the Eu^{III} ion is nine and that a guest water molecule is encapsulated in the cavity. The cryptates have a high stability which confers good fluorescence properties in solution.

Introduction

Studies on the syntheses and properties of lanthanide macrocyclic complexes are a fascinating area.[1,2] Their novel structures and interesting properties make macrocyclic lanthanide complexes valuable for technological applications.[3–5] Europium(III) complexes, for instance, can be used as luminescence probes in biology,[6–9] as luminescence labels in medical diagnostics,[10,11] and as contrast agents for magnetic resonance imaging.[12,13] Recent research has demonstrated that cryptands are useful as potential ligands for encapsulating lanthanide(III) ions and are able to shield metal ions from interaction with solvents to avoid radiationless deactivation processes in luminescence emission. Cryptates have high thermodynamic and kinetic stability and metal ion dissociation is negligible at high dilution.

Lanthanide cryptates with valuable luminescence properties can be obtained by a suitable choice of ligands with antenna chromophores.[1] Recently, the syntheses and metal luminescence properties of some cryptates have been reported, such as the cryptates based on oxamacrocycles,[14,15] azamacrocycles,[16,17] macrocycles with bipyridyl[18,19] and phenanthroline groups,[20] and macrocycles with functionalized calixarenes.[21,22] However, the number and type of cryptates are still quite limited.[23] A new kind of lanthanide cryptate (Gd^{III}, Tb^{III}, Eu^{III} and Dy^{III} etc.) derived from tris(2-aminoethyl)amine (tren) and 2,6-diformylphenol (dfp) was reported previously by Nelson,[24] Fenton[25] and our group,[26] although their luminescence properties were hardly mentioned. Recently, Plates et al.[27] made a detailed study on the solid fluorescence of phenolic cryptates of Eu, Dy, Yb; in solution; their fluorescence, however, is quenched completely by nonradiative deactivation. Herein we report some europium(III) and terbium(III) cryptates derived from the reaction of tren with 2,6-diformyl-4-R-phenol [R = Cl (dcp), F (dfp), *t*Bu (dbp)] (Figure 1). Their compositions and structures are slightly different from those previously reported[24,25] due to different reaction conditions. They possess a high coordination number (nine), a water molecule encapsulated in the inner sphere of the complex as a guest (not coordinated to the metal ion), and a high stability. These features result in their good fluorescence properties in solutions.

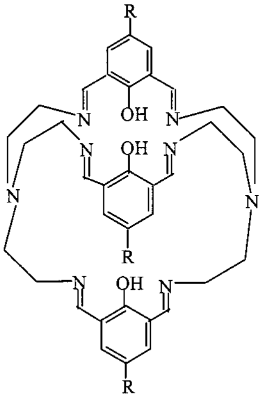

Figure 1. The chemical formula of H_3L [L^1, R = Cl; L^2, R = F; L^3, R = $C(CH_3)_3$]

Results and Discussion

Characterization of the Cryptates

According to the elemental analyses and molar conductivities (Table 1), the cryptates can be divided into three kinds: (a) 1:1 electrolytes $[Ln(H_2L^1)(NO_3)(H_2O)]NO_3$ [Ln = Eu^{III} **2**; Tb^{III} **3**]; (b) 2:1 electrolytes $[Eu(H_3L^1)(NO_3)(H_2O)](NO_3)_2$ **1**; (c) double salts (1:1 electrolytes) $[Ln(H_2L^{2,3})(NO_3)(H_2O)][Ln(NO_3)_4]$ (Ln = Eu^{III}, Tb^{III}, **4–7**]. The type of complex obtained was determined chiefly by the reaction conditions. For example, when using excess tren (i.e. a molar ratio tren:dfp (or dcp):Ln^{III} of 2:2:1), the phenolic protons were neutralized because of the slight basicity of the solution and the 1:1 electrolytes were obtained; when the molar ratio of the three materials is 2:3:1, the

---

[a] Coordination Chemistry Institute and State Key Laboratory of Coordination Chemistry, Nanjing University,
Nanjing 210093, P. R. China

1434–1948/01/0404–1063 $ 17.50+.50/0

Table 1. Elemental analysis and molar conductance data for the cryptates

No.	Cryptate (Formula)[a]	Yield (%)	Analysis(%) C, H, N[b]	Λ_m (298 K) scm^{2}mol (DMF)
1	$[Eu(H_3L^1)(NO_3)(H_2O)](NO_3)_2$ $(C_{36}H_{41}Cl_3EuN_{11}O_{13})$	65	39.30, 4.01, 13.45 (39.90), (3.87), (13.86)	125
2	$[Eu(H_2L^1)(NO_3)(H_2O)](NO_3)\cdot 4H_2O$ $(C_{36}H_{48}Cl_3EuN_{10}O_{14})$	73	38.78, 4.35, 12.34 (39.18), (4.35), (12.70)	88
3	$[Tb(H_2L^1)(NO_3)(H_2O)](NO_3)\cdot 9H_2O$ $(C_{36}H_{58}Cl_3N_{10}O_{19}Tb)$	68	35.80, 4.79, 11.77 (36.03), (4.87), (11.67)	81
4	$[Eu(H_2L^2)(NO_3)(H_2O)][Eu(NO_3)_4]\cdot 2H_2O$ $(C_{36}H_{44}Eu_2F_3N_{13}O_{21})$	58	31.72, 3.62, 13.30 (31.86), (3.30), (13.40)	65
5	$[Tb(H_2L^2)(NO_3)(H_2O)][Eu(NO_3)_4]\cdot 3H_2O$ $(C_{36}H_{46}F_3N_{13}O_{22}Tb_2)$	52	30.72, 3.32, 13.51 (31.14), (3.34), (13.12)	84
6	$[Eu(H_2L^3)(NO_3)(H_2O)][Eu(NO_3)_4]\cdot 3H_2O$ $(C_{48}H_{73}Eu_2N_{13}O_{21})$	48	38.84, 4.77, 12.68 (39.16), (4.94), (12.37)	84
7	$[Tb(H_2L^3)(NO_3)(H_2O)][Tb(NO_3)_4]\cdot 4H_2O$ $(C_{48}H_{75}N_{13}O_{22}Tb_2)$	47	38.40, 5.32, 12.46 (38.37), (5.02), (12.13)	81

[a] H_3L^1, H_2L^2, H_2L^3 denote the cryptand; the subscripts of H denote the number of protons on the phenoxy group in the cryptand. − [b] Calculated values for the formula of cryptates are given in parentheses.

2:1 electrolyte was produced; when excessive lanthanide(III) nitrate was added the double salts were obtained. Our one-step synthesis is quite different from the two-step procedure which includes the preparation of sodium complexes and a subsequent transmetallation reaction. In our cryptates, the coordination entities are also quite different from those of other authors[24,25,38] (see below).

The IR spectra of the cryptates (Table 2) show a band at ca. 1650 cm^{-1} attributable to ν(C=N). The bands at 1478 cm^{-1} and 1296 cm^{-1} are due to ν(N=O) (ν_1) and $\nu_{aym}(NO_2)$ (ν_5), respectively, of the coordinated nitrate. The $\nu_{sym}(NO_2)$ vibration (ν_2) at 1051 cm^{-1} is characteristic of a bidentate nitrate group. The strong sharp band at 1384 cm^{-1} is characteristic of an ionic nitrate.[36] The IR spectra show that there are both coordinated and ionic nitrates in the complexes.

The electronic spectra of the cryptates display three strong absorption bands. The band centered around 400 nm is assigned to the C=N chromophores, whereas the other two bands at ca. 270 nm and 230 nm are assigned to the π−π* transition of the K band of the benzene rings.

Thermogravimetric analysis of $[Eu(H_3L^1)(NO_3)(H_2O)](NO_3)_2$ shows that there are three weight-loss processes. The cryptate begins to lose 1.55% of its weight below 120 °C, corresponding to the loss of one water molecule (calcd. 1.65%), indicating that the water molecule in the cavity is only weakly bound. The second step occurs at 210−310 °C, where 11.1% of the total weight was lost, corresponding to the loss of the two nitrate ions in the outer sphere (calcd. 11.34%). In the range 311−340 °C, a weight loss of 5.8% is observed due to loss of the coordinated nitrate ion (calcd. 5.67%).

Electrospray Mass Spectrum

The positive-ion ES mass spectrum of $[Eu(H_2L^1)(NO_3)(H_2O)]^+$ is shown in Figure 2. The base peak at *m*/*z* = 887.5 corresponds to $[Eu(HL^1)]^+$ $(C_{36}H_{37}Cl_3EuN_8O_3)$ whose isotopic distribution is shown in Figure 3a. From the numbers and natural isotopic abundances of the atoms in $[Eu(HL^1)]^+$, a revised program[37] was used to calculate the isotopic distribution at *m*/*z* = 887.5. The calculated pattern (Figure 3b) agrees well with the experimental one. The other peaks in Figure 2 can be assigned to the species formed by solvation, loss of protons and loss of the chlorine atoms from the benzene ring of the cryptate. The ES-MS peaks of the representative cryptates are shown

Table 2. IR and UV spectroscopic data for the cryptates **1−7**

Cryptate	IR						UV(MeCN)		
	O−H	C=N	N=O	ν_{max} (cm^{-1}) NO_3^-	$NO_{2\ (asymm)}$	$NO_{2\ (sym)}$	λ_{max} (nm) (ε/dm^{3}mol^{-1}cm^{-1})		
1	3380	1650s 1640s	1478s	1384s	1296s	1051s	230 (83000)	264 (30000)	406 (16000)
2	3381	1653s	1478s	1384s	1297s	1050s	226 (86000)	269 (31000)	412 (13000)
3	3400	1645s	1475s	1384s	1292s	1060s	228 (96000)	268 (37000)	412 (18000)
4	3380	1655s	1478s	1384s	1290s	1040s	229 (79000)	272 (39000)	408 (25000)
5	3384	1645s	1475s	1384s	1292s	1040s	225 (58000)	272 (45000)	412 (33000)
6	3410	1642s	1478s	1384s	1296s	1042s	228 (73000)	267 (42000)	410 (10000)
7	3402	1640s	1478s	1384s	1296s	1041s	228 (94000)	251 (33000)	410 (12000)

in Table 3. The base peaks of the three cryptates formed by losing the encapsulated water molecule and the coordinated nitrate anion, namely $[Ln(H_nL)]^{n+}$, are different from those of the Nd^{III} cryptates,[26] with a base peak corresponding to $[Nd(HL^1)(NO_3)(H_3O)]^+$, indicating that under similar ES-MS conditions, the encapsulated water molecule and the coordinated nitrate anion in $[Eu(H_3L^1)(NO_3)(H_2O)]^{2+}$ can be lost easier than those in $[Nd(HL^1)(NO_3)(H_3O)]^+$. This may be due to the different distances between the water molecule and the metal atom in the cavity. In the cryptate **1** the distance for Eu−O(1w) is 3.070 Å, which is longer than the Nd−O(oxonium) bond (3.027 Å), as shown by X-ray structural analysis.

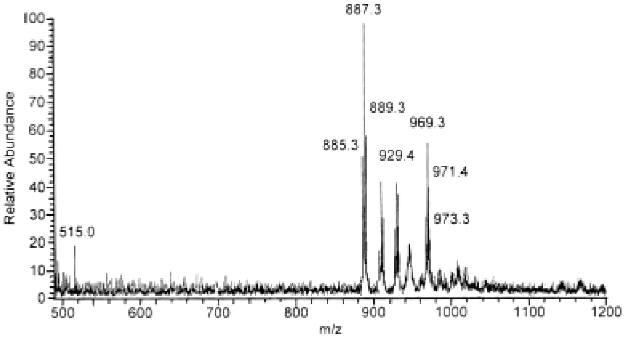

Figure 2. The ES-MS spectrum of the $[Eu(H_2L^1)(NO_3)(H_2O)]^+$ in MeOH

Crystal Structure

The structure of the cryptate cation $[Eu(H_3L^1)(NO_3)(H_2O)]^{2+}$ is shown in Figure 4. The crystal structure data are listed in Table 4 and 5. In the complex, Eu^{III} is located asymmetrically at one end of the cavity and is nine-coordinated, by three imino nitrogen atoms N(3), N(6), N(8), three phenolic oxygens O(1), O(2), O(3), two oxygens of the bidentate nitrate O(4), O(5) and one of the bridgehead nitrogen atoms, and forms a distorted monocapped square antiprism. The coordination distances are 2.491 and 2.532 Å, respectively, for two oxygens of the bidentate nitrate, in the range 2.288−2.416 Å for the phenolic oxygens, 2.492−2.562 Å for the imino nitrogens, and the Eu^{III}−N(4) distance is 2.761 Å, showing a weak interaction between Eu^{III} and the bridgehead nitrogen atom. Except for the coordination distance of Eu^{III}−N(4), the other bond distances are shorter than those of the Nd^{III} cryptate containing the same ligand.[26] This may be because the Eu^{3+} ion has a smaller radius than Nd^{3+}. In the distorted, capped, square antiprism, N(4) is the capped atom and the four oxygen atoms O(1), O(2), O(3), O(4) form the distorted basal plane (mean deviation 0.1862 Å); the distance between Eu^{III} and the basal plane is 1.3602 Å. The upper plane is composed of N(3), N(6), N(8) and O(5) (mean deviation 0.0776 Å), and the distance between the upper plane and Eu^{III} is 0.9551 Å. The biplanar angle between the two planes is 5.2°. The distance between the two bridgehead nitrogens N(1) and N(4) is 8.407 Å.

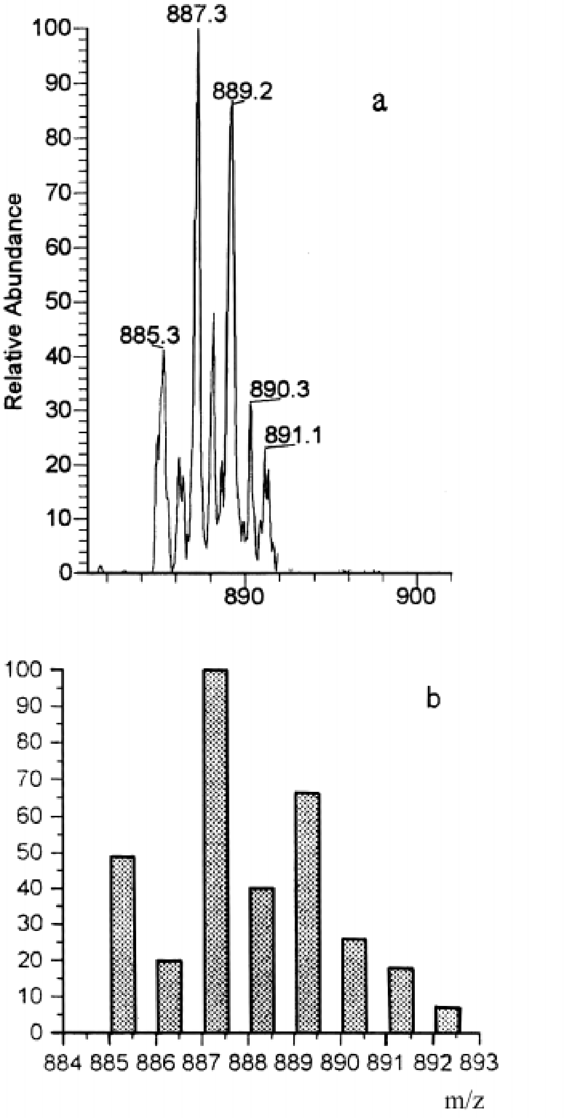

Figure 3. The isotopic distribution of the peak cluster at *m/z* = 887.5 for $[Eu(H_2L^1)(NO_3)(H_2O)]^+$: (a) experimental pattern, (b) calculated pattern

At one end of the cavity, a water molecule is encapsulated in the host macrocycle as a guest; the distance between O(1w) of the water molecule and Eu^{III} is 3.070 Å, and is longer than that of reported analogous cryptates whose distances are in the range 2.304−2.437 Å.[24,38] This confirms that the water molecule in our cryptate is not coordinated to the Eu^{III} atom.

Luminescence Properties of the Cryptates

Excitation of the Eu^{III} cryptates in MeCN solution with light at 400 nm gives rise to the characteristic emission of the Eu^{3+} ion and all four cryptates have similar emission spectra. Comparing the excitation band with the absorption band of the cryptate **2** at ca. 400 nm, the similarity between the absorption and excitation spectra indicates energy transfers from the excited state of the ligand to the Eu^{III} vibration level.[6] The emission spectrum of the cryptate **2**

Table 3. ES-MS spectroscopic data for the cryptates **2**, **6** and **7** in methanol solution

	Cryptate	Peak (*m*/*z*)	Assignment
2	$[Eu(H_2L^1)(NO_3)(H_2O)]^+$	969.5 (60)	$[Eu(H_2L^1)(NO_3)(H_2O)]^+$
		947.5 (25)	$[Eu(H_2L^{1-}2Cl)(NO_3)(H_2O)_2+MeOH]^+$
		929.5 (55)	$[Eu(H_2L^{1-}2Cl)(NO_3)(H_2O)+MeOH]^+$
		887.5 (100)	$[Eu(HL^1)]^+$
		515.0 (20)	$[Eu(H_3L^1\text{-}Cl)(NO_3)(H_2O)+3MeOH]^{2+}$
6	$[Eu(H_2L^3)(NO_3)(H_2O)]^+$	975.4 (45)	$[Eu(HL^3\text{-}C(CH_3)_3](NO_3)(H_2O)]^+$
		952.5 (100)	$[Eu(HL^3)]^+$
		476.8 (30)	$[Eu(H_2L^3)]^{2+}$
7	$[Tb(H_2L^3)(NO_3)(H_2O)]^+$	1022.2 (24)	$[Tb(H_2L^3)(NO_3)]^+$
		959.4 (48)	$[Tb(HL^3)]^+$
		511.7 (14)	$[Tb(H_3L^3)(NO_3)]^{2+}$
		480.2 (100)	$[Tb(H_2L^3)]^{2+}$

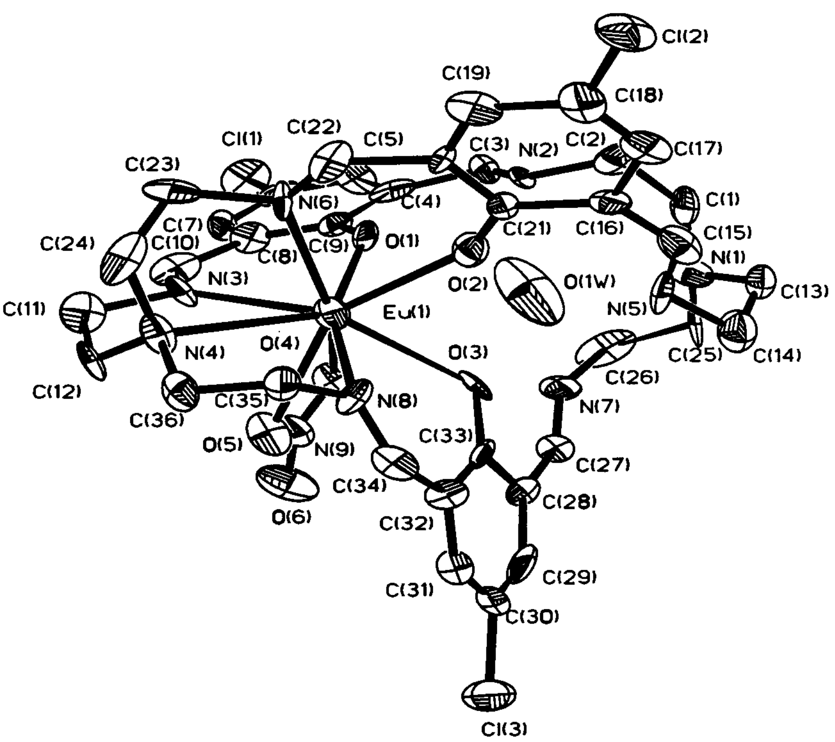

Figure 4. Crystal structure of $[Eu(H_3L)(NO_3)(H_2O)]^{2+}$ ion

is shown in Figure 5. All emissions arise from the $^5D_0$ level corresponding to the $^5D_0 \rightarrow {}^7F_1$ ($\Delta J = 0, 1-4$) transition. The weak band at 580 nm arises from the $^5D_0 \rightarrow {}^7F_0$ transition. The band around 593 nm for $^5D_0 \rightarrow {}^7F_1$, which is magnetic-dipole allowed, is hardly affected by a change of the coordination environment. The intense band around 613 nm for $^5D_0 \rightarrow {}^7F_2$ is an electric-dipole allowed transition and its emission intensity is sensitive to the coordination environment of Eu^{III}. The intensity for the $^5D_0 \rightarrow {}^7F_2$ transition is much higher than that for $^5D_0 \rightarrow {}^7F_1$, showing that the complex has no inversion center. All the ratios of the intensities of the $^5D_0 \rightarrow {}^7F_2$ to the $^5D_0 \rightarrow {}^7F_1$ transition are about 4.5:1 for the three cryptates (**2**, **4** and **6**) with different substituents, implying a similar symmetry.[23] The bands around 655 nm and the bands around 700 nm are produced from the transitions $^5D_0 \rightarrow {}^7F_3$ and $^5D_0 \rightarrow {}^7F_4$, respectively. A wide band around 480 nm is observed corresponding to the ligand emission whose quantum yield is 8.8×10^{-2} (MeCN).

Under the same experimental conditions, the Tb^{III} cryptate **7** displays a weak band at 542 nm, due to the $^5D_4 \rightarrow {}^7F_5$ transition, which is overlapped partly by a strong emission band of the ligand. For cryptates **3** and **5**, only a ligand-centered band is observed, implying a poor energy transfer between the ligand triplet state and the $^5D_4$ state of Tb^{III}.

The luminescent quantum yields and the life times at 613 nm of some Eu^{III} cryptates in MeCN are shown in Table 6. From this table it can be seen that the quantum yield and lifetime of the cryptate **2** with a chlorine substituent are higher than those of **3** and **6**. The reason for this is not clear yet as there are very few of these cryptates with which to make a good comparison.

Table 4. Crystal data and structure refinement

Formula	$C_{36}H_{41}Cl_3EuN_{11}O_{13}$
M_r	1091.11
Color/habit	Orange, block
Crystal system	Orthorhombic
Space group	*Pbca*
a (Å)	16.987(7)
b (Å)	20.688(5)
c (Å)	24.641(6)
V (Å^3)	8659.3(47)
Z	8
$D_{\mathrm{calcd.}}$ (Mg m^{-3})	1.678
$F(000)$	4416
Crystal dimensions	0.4 × 0.3 × 0.3
Mo-K_α radiation (Å)	0.71073
2θ range (°)	1.76 to 22.50
Absorption coefficient (mm^{-1})	1.710
Index ranges	$-1 \le h \le 18$ $-1 \le k \le 22$ $-1 \le l \le 26$
Reflection collected	6866
Independent reflections	5663
Observed reflections	2115
R, wR (observed data)	0.0768, 0.1303
w^{-1}	$\sigma^2(F_0)^2 + (0.0000P)^2 + 0.0000P$ $P = [(F_0)^2 + 2(F_c)^2]/3$
Goodness of fit	1.004
Largest difference peak (eÅ^{-3})	0.956
Largest difference hole (eÅ^{-3})	−0.740

Table 5. Selected bond lengths (Å) and angles (°) for cryptate **1**

Eu(1)−O(1)	2.288(6)	Eu(1)−O(2)	2.374(6)
Eu(1)−O(3)	2.418(6)	Eu(1)−N(8)	2.492(7)
Eu(1)−O(5)	2.491(7)	Eu(1)−N(3)	2.532(7)
Eu(1)−N(6)	2.562(7)	Eu(1)−O(4)	2.649(7)
Eu(1)−N(4)	2.761(7)		
C(15)−N(5)	1.334(12)	C(22)−N(6)	1.260(11)
C(3)−N(2)	1.242(12)	C(34)−N(8)	1.289(12)
C(27)−N(7)	1.185(12)	C(10)−N(3)	1.281(12)
O(1)−Eu(1)−O(2)	78.5(2)	O(1)−Eu(1)−O(3)	97.9(2)
O(2)−Eu(1)−O(3)	70.8(2)	O(1)−Eu(1)−N(8)	160.7(2)
O(2)−Eu(1)−N(8)	83.8(2)	O(3)−Eu(1)−N(8)	68.7(2)
O(1)−Eu(1)−O(5)	118.9(2)	O(2)−Eu(1)−O(5)	144.2(2)
O(3)−Eu(1)−O(5)	75.7(2)	N(8)−Eu(1)−O(5)	72.5(2)
O(1)−Eu(1)−N(3)	71.3(2)	O(2)−Eu(1)−N(3)	140.4(2)
O(3)−Eu(1)−N(3)	137.4(2)	N(8)−Eu(1)−N(3)	127.9(2)
N(8)−Eu(1)−N(3)	128.1(2)	O(5)−Eu(1)−N(3)	74.6(2)
O(1)−Eu(1)−N(6)	87.1(2)	O(2)−Eu(1)−N(6)	66.9(2)
O(3)−Eu(1)−N(6)	135.4(2)	N(8)−Eu(1)−N(6)	93.1(2)
O(5)−Eu(1)−N(6)	139.0(2)	N(3)−Eu(1)−N(6)	86.2(2)
O(1)−Eu(1)−O(4)	71.0(2)	O(2)−Eu(1)−O(4)	124.2(2)
O(3)−Eu(1)−O(4)	68.7(2)	N(8)−Eu(1)−O(4)	114.1(2)
O(5)−Eu(1)−O(4)	49.7(2)	N(3)−Eu(1)−O(4)	68.8(2)
N(6)−Eu(1)−O(4)	150.7(2)	O(1)−Eu(1)−N(4)	130.4(2)
N(8)−Eu(1)−N(4)	66.0(2)	O(5)−Eu(1)−N(4)	73.9(2)
N(3)−Eu(1)−N(4)	66.8(2)	N(6)−Eu(1)−N(4)	65.2(2)
O(4)−Eu(1)−N(4)	114.8(2)	O(3)−Eu(1)−N(4)	130.9(2)
O(2)−Eu(1)−N(4)	120.5(2)		

The fluorescence properties of the europium(III) cryptates derived from 2,6-diformylphenol have attracted much attention. These studies have focused on the cryptates with CH_3, OCH_3 and phenyl substituents,[27,38] although they do not display fluorescent emission in solution. The luminescence difference between our cryptates and other authors' ones results from the different structures. As shown by the crystal structure, the coordination number of Eu^{III} in cryptate **1** is nine, and in **2**−**7** it is also nine. Coordinative saturation of Eu^{III} blocks the coordination of solvent molecules to the metal centre. It is of interest to note that, for **1**, the water molecule does not coordinate to Eu^{III} even though it is located within the cryptate cavity. This is not the case for the Eu^{III} phenolic cryptates reported by other authors,[24,25,38] in which coordination numbers of seven or eight, and a water molecule or monodentate ligand, which can dissociate easily (SCN^-,NO_3^-, etc.), are found coordinated to the metal ion. In these cases, in solution, the interaction between the Eu^{III} and water or solvent molecules results in nonradiative deactivation which quenches the fluorescence.

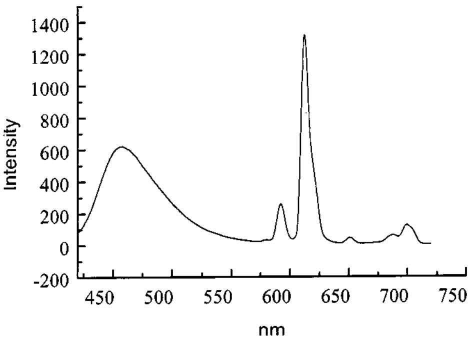

Figure 5. Emission spectra for the cryptate **2** in MeCN at an excitation wavelength of 400 nm

Table 6. Luminescent quantum yield(Φ) and lifetime (τ) of the mononuclear Eu^{III} complexes in MeCN solution at 293 K

Complex	$\Phi_{\mathrm{Eu}^{III}} \times 10^{2}$[a], [b]	τ (ms)
2	4.3	0.88
3	0.20	0.51
6	0.24	−

[a] Excitation at 400 nm; concentration of Eu^{III}complexes is 2×10^{-6} M. − [b] Experimental errors ± 20%.

Experimental Section

Materials: $Ln(NO_3)_3 6H_2O$ (Ln = Eu, Tb) was prepared by dissolving Ln_2O_3 (99.99%) in an excess of nitric acid; 2,6-diformyl-4-R-phenol (R = Cl, F, *t*Bu)[28] and tris(2-aminoethyl)amine (tren) were prepared by literature methods.[29] Their physical constants and spectroscopic data are in agreement with literature values. The acetonitrile for the fluorescence study was dried by treatment with CaH_2 and distillation over P_2O_5. The $[Ru(bipy)_3]Cl_2$ used as a standard material in the quantum yield measurement was synthesized according to a literature procedure[30] and recrystallized twice from doubly distilled water. Its spectroscopic data were in agreement with literature values; its quantum yield value was checked against rhodamine B[31] and was also in accordance with the literature value.

Physical Measurements: Elemental analysis was performed on a Perkin−Elmer 240c analytical instrument. The molar electrical conductivitives in DMF solution containing $\approx 10^{-4}$ mol dm^{-3} complexes were measured at 25 °C ± 0.1 °C using a BSD-A conductometer. The IR spectra were measured as a KBr disc using a Nicolet 5 DX FT-IR spectrophotometer. Electronic spectra were recorded on a UV-3100 spectrophotometer. Thermoanalysis of the complexes was performed on a SDT 2960C TA thermoanalyser under an argon atmosphere at a rate of 10 °C $\min^{-1}$. The electrospray mass spectra (ES-MS) were determined on a Finnigan LCQ mass spectrometer; the concentrations of the samples were about 1.0 μmol dm^{-3}. The diluted solutions were electrosprayed at a flow rate of 5×10^{-6} dm^{-3} $\min^{-1}$ with a needle voltage of +4.5 kV. The mobile phase was an aqueous solution of methanol (v/v, 1:1). The samples were run in the positive-ion mode.

Luminescence Measurement: The luminescence spectra were measured with a Hiachi Model F4500 spectrofluorometer. In measurements of emission and excitation spectra the bandpass was 5.0 nm. The quantum yield of the Eu^{III} complexes was measured using a relative method with $[Ru(bipy)_3]Cl_2$ as the standard. Its quantum yield is 0.042 in aqueous solution at 20 °C.[35] The quantum yields of the Eu^{III} complexes were calculated from Equation (1):

$$\Phi_x/\Phi_s = [A_s/A_x]\,[n_x^2/n_s^2][D_x/D_s] \qquad (1)$$

where Φ is the quantum yield, subscript s stands for the reference and x for the sample, A is the absorbance at the excitation wavelength, *n* is the refractive index (1.343 for MeCN solution and 1.344 for aqueous solution),[31] and *D* is the emission integrated area. The sample absorbances at excitation wavelength were kept as low as possible to avoid fluorescence errors ($A_{exc} = 0.09-0.11$). Solutions containing complexes of about 1.0×10^{-6} mol dm^{-3} were deoxygenated with a stream of super-pure nitrogen for 15 minutes.

The fluorescence lifetimes of the complexes were measured on a SPEX-FL2T2 spectrofluorimeter equipped with a flash lamp. The signals were recorded by photomultiplier using single-photon counting. Because in each solution only a single light-emitting species is present and there is no quenching of the emissive state by other excited state molecules, the fluorescence intensities decay exponentially over time *t*, obeying Equation (2):[34]

$$I_t = I_0 \exp(-t/\tau) \qquad (2)$$

where I_0 and I_t are the fluorescence intensities at the time t = 0 and time t, respectively. The emission lifetime of fluorescence, τ, was obtained by fitting the fluorescence-decay curve into Equation (2).

Crystal Structure Determination: A summary of the crystal data, intensity collection and structure refinement is given in Table 4. Intensity data were measured on a Siemens P4 four-circle diffractometer with monochromatic Mo-K_α (λ = 0.71073) radiation in the ω-scan mode with a variable scan speed of 4.0−60.0° $\min.^{-1}$ in ω. All data were corrected for Lorentz and polarization effects during data reduction using XSCANS.[32]

The structure was solved by direct methods. All non-hydrogen atoms were refined anisotropically by full-matrix least-squares. The hydrogen atoms of the ligands were placed in their calculated positions with C−H = 0.93 Å. The hydrogen atoms of the water molecules in the cryptate **1** were found in the difference Fourier map. All the hydrogen atoms were assigned fixed isotropic thermal parameters (1.2 times that of the atoms to which they are attached) and allowed to ride on their respective parent atoms. The contributions of these hydrogen atoms were included in the structure-factor calculations. One of the two nitrate anions was found to be disordered. The s.o.f.'s were 0.54 and 0.46 for the disordered parts containing nitrogen atoms N(11) and N(11′), respectively. All computations were carried out using the SHELXTL-PC program package.[33]

Syntheses of the Cryptates

$[Eu(H_3L^1)(NO_3)(H_2O)](NO_3)_2$ (1): A methanol solution (10 cm^3) containing tren (0.058 g, 0.40 mmol) was added dropwise to a stirred methanol solution (15 cm^3) containing dcp (0.111 g, 0.6 mmol) and $Eu(NO_3)_3{\cdot}6H_2O$ (0.112 g, 0.25 mmol). The reaction mixture was refluxed for 4 hours. Concentration of the solution resulted in the yellowish product $[Eu(H_3L^1)(NO_3)(H_2O)](NO_3)_2$ which was filtered off, washed with methanol and diethyl ether, and dried in a vacuum desiccator.

The cryptates **2**−**7** were prepared by a similar procedure except that the molar ratios were changed. For **2** and **3**: tren:dcp:Eu^{3+} = 1:1.2:0.5; for **4**−**7**: tren:dfp (or dbp):Eu^{3+} = 1:1.2:1.

Acknowledgments

The work was supported by the National Natural Science Foundation and the 211 project of China.

---

[1] V. Alexander, *Chem. Rev.* **1995**, *95*, 237−342.
[2] J.-M. Lehn, *Angew. Chem. Int. Ed. Engl.* **1990**, *29*, 1304−1319.
[3] N. Sabbatini, M. Guardigi, *Coord. Chem. Rev.* **1993**, *123*, 201−228.
[4] G. R. Choppin, D. R. Peterman, *Coord. Chem. Rev.* **1998**, *174*, 283.
[5] P. Ghosh, P. K. Bharadwaj, J. Roy. S. Ghosh, *J. Am. Chem. Soc.* **1997**, *119*, 11903−11909.
[6] D. Parker, J. A. G. Williams, *J. Chem. Soc., Dalton Trans.* **1996**, 3613−3628.
[7] F. Richardson, *Chem. Rev.* **1982**, *82*, 541−552.
[8] G. Mathis, *Clin. Chem. (Washington, D.C.)* **1993**, *39*, 1953−1959.
[9] E. Soini, I. Hemmila, *Clin. Chem.* **1979**, *25*, 353−358.
[10] J. L. Toner, in *Inclusion Phenomena and Molecular Recognition* (Ed.: J. Atwood), Plenum Press, New York, **1990**, p 185.
[11] C. H. Evans, *Biochemistry of the Elements*, vol. 8 ("Biochemistry of the Lanthanides"), Plenum, New York, N.Y., **1990**.
[12] P. Caravan, J. J. Ellison, T. J. McMurry, R. B. Lauffer, *Chem. Rev.* **1999**, *99*, 2293−2353.
[13] [13a]P. R. Selvin, T. M. Rana, J. E. Hearst, *J. Am. Chem. Soc.* **1994**, *116*, 6029−6030. − [13b] R. Edelman, S. Warach, *New Eng. J. Med.* **1993**, *328*, 708−714.
[14] B. Alpha, E. Anklam, R. Deschenaux, J.-M. Lehn, M. Pietraszkiewicz, *Helv. Chim. Acta.* **1988**, *71*, 1042−1052.
[15] J.-M. Lehn, M. Pietraszkiewicz, J. karpiuk, *Helv. Chim. Acta.* **1990**, *73*, 106−111.
[16] L. Prodi, M. Maestri, R. Ziessei, V. Balzani, *Inorg. Chem.* **1991**, *30*, 3798−3802.
[17] F. Bodar−Houillon, A. Marsura, *New. J. Chem.* **1996**, *20*, 1041−1045.
[18] N. Sabbatini, M. Guardigilli, I. Manet, F. Bolletta, *Inorg. Chem.* **1994**, *33*, 955−959.
[19] V. Balzani, J.-M. Lehn, J. Van De Loosdrecht, A. Mecati, N. Sabbatini, R. Ziessel, *Angew. Chem. Int. Ed. Engl.* **1991**, *30*, 190−191.
[20] K. Sasamoto, *European Patent*, EP. 0,493,745 AI. **1991**.
[21] H. Matsumoto, S. Shinkai, *Chem. Lett.* **1994**, 901−904.
[22] F. J. Steemer, W. Verboom, D. N. Reinhoudt, E. B. Van Der Tol, J. W. Verhoeven, *J. Am. Chem. Soc.* **1995**, *117*, 9408−9414.
[23] C. Galaup, C. Picard, B. Cathala, L. Cazaux, P. Tisnes, H. Autiero, D. Aspe, *Helv. Chim. Acta* **1999**, *82*, 543−560.
[24] M. G. B. Drew, O. W. Howarth, C. J. Harding, N. Martin, J. Nelson, *J. Chem. Soc., Chem. Commun.* **1995**, 903−905.
[25] F. Avecilla, R. Bastida, A. de Blas, D. E. Fenton, A. Macias, A. Rodriguez, T. Rodriguez-Blas, S. Garcia-Granda, R. Corza-Suarez, *J. Chem. Soc., Dalton Trans.* **1997**, 409−415.
[26] [26a] C.-J. Feng, Q.-H. Luo, C.-Y. Duan, M.-C. Shen, Y.-J. Liu, *J. Chem. Soc., Dalton Trans* **1998**, 1377−1380. − [26b] J.-J.

Zhang, W. Zhang, Q.-H. Luo, Y.-H. Mei, *Polyhedron* **1999**, *18*, 3637−3642.

[27] C. Platas, F. Avecilla, A. de Blas, T.Rodrigues−Blas, C. F. G. C. Geraldes, E. Toth, A. E. Merbach, J.-C. G. Bunzli, *J. Chem. Soc., Dalton Trans.* **2000**, 611−618.

[28] E. Kimura, S. Young, J. P. Collman, *Inorg, Chem.* **1970**, *9*, 118−124.

[29] S. Taniguchi, *Bull. Chem. Soc. Jpn.* **1984**, *57*, 2683−2684.

[30] F. H. Burstall, *J. Chem. Soc.* **1936**, *1*, 173−175.

[31] K.Nakamaru, *Bull. Chem. Soc. Jpn.* **1982**, 2697−2705.

[32] XSCANS (Version 2.1), Siemens Analytical X-ray Instruments, Inc., Madison, WI, **1994**.

[33] SHELXTL (Version 5.0), Siemens Industrial Automation, Inc., Analytical Instrumentation, Madison, WI. **1995**.

[34] D. E. Eaton, *Pure Appl. Chem.* **1988**, *60*, 1107−1114.

[35] J. V. Houten, R. J. Watts, *J. Am. Chem. Soc.* **1976**, *98*, 4853−4858.

[36] K. Nakampto, *Infrared and Raman Spectra of Inorganic and Coordination Compounds* 3rd ed., Wiley−Interscience, New York, **1978**.

[37] J. D. Tee, *Talanta* **1973**, *20*, 1029−1038.

[38] S.-Y. Yu, Q. Huang, B. Wu, W.-J. Zheng, X.-T. Wu, *J. Chem. Soc., Dalton Trans.* **1996**, 3883−3888.

Received September 12, 2000
[I00343]